

4-1-2010

# Dysautonomia Due to Reduced Cholinergic Neurotransmission Causes Cardiac Remodeling and Heart Failure

Aline Lara

*Universidade Federal de Minas Gerais*

Denis D. Damasceno

*Universidade Federal de Minas Gerais*

Rita Pires

*Western University*

Robert Gros

*Western University*

Eneas R. Gomes

*Universidade Federal de Minas Gerais*

*See next page for additional authors*

Follow this and additional works at: <https://ir.lib.uwo.ca/anatomypub>

 Part of the [Anatomy Commons](#), and the [Cell and Developmental Biology Commons](#)

---

## Citation of this paper:

Lara, Aline; Damasceno, Denis D.; Pires, Rita; Gros, Robert; Gomes, Eneas R.; Gavioli, Mariana; Lima, Ricardo F.; Guimaraes, Diogo; Lima, Patricia; Bueno, Carlos Roberto Jr; Vasconcelos, Anilton; Roman-Campos, Danilo; Menezes, Cristiane A. S.; Sirvente, Raquel A.; Salemi, Vera M.; Mady, Charles; Caron, Marc G.; Ferreira, Anderson J.; Brum, Patricia C.; Resende, Rodrigo R.; Cruz, Jader S.; Gomez, Marcus Vinicius; Prado, Vania F.; de Almeida, Alvair P.; Prado, Marco A. M.; and Guatimosim, Silvia, "Dysautonomia Due to Reduced Cholinergic Neurotransmission Causes Cardiac Remodeling and Heart Failure" (2010). *Anatomy and Cell Biology Publications*. 35.

<https://ir.lib.uwo.ca/anatomypub/35>

---

**Authors**

Aline Lara, Denis D. Damasceno, Rita Pires, Robert Gros, Eneas R. Gomes, Mariana Gavioli, Ricardo F. Lima, Diogo Guimaraes, Patricia Lima, Carlos Roberto Bueno Jr., Anilton Vasconcelos, Danilo Roman-Campos, Cristiane A. S. Menezes, Raquel A. Sirvente, Vera M. Salemi, Charles Mady, Marc G. Caron, Anderson J. Ferreira, Patricia C. Brum, Rodrigo R. Resende, Jader S. Cruz, Marcus Vinicius Gomez, Vania F. Prado, Alvair P. de Almeida, Marco A. M. Prado, and Silvia Guatimosim

## Dysautonomia Due to Reduced Cholinergic Neurotransmission Causes Cardiac Remodeling and Heart Failure<sup>∇‡</sup>

Aline Lara,<sup>1†</sup> Denis D. Damasceno,<sup>1†</sup> Rita Pires,<sup>2†</sup> Robert Gros,<sup>2,8†</sup> Enéas R. Gomes,<sup>1</sup> Mariana Gavioli,<sup>1</sup> Ricardo F. Lima,<sup>1</sup> Diogo Guimarães,<sup>1</sup> Patricia Lima,<sup>3</sup> Carlos Roberto Bueno, Jr.,<sup>4</sup> Anilton Vasconcelos,<sup>5</sup> Danilo Roman-Campos,<sup>7</sup> Cristiane A. S. Menezes,<sup>2</sup> Raquel A. Sirvente,<sup>11</sup> Vera M. Salemi,<sup>11</sup> Charles Mady,<sup>11</sup> Marc G. Caron,<sup>6</sup> Anderson J. Ferreira,<sup>3</sup> Patricia C. Brum,<sup>4</sup> Rodrigo R. Resende,<sup>10</sup> Jader S. Cruz,<sup>7</sup> Marcus Vinicius Gomez,<sup>12</sup> Vania F. Prado,<sup>2,8,9</sup> Alvaír P. de Almeida,<sup>1</sup> Marco A. M. Prado,<sup>2,8,9\*</sup> and Silvia Guatimosim<sup>1\*</sup>

*Departments of Physiology and Biophysics,<sup>1</sup> Morphology,<sup>3</sup> Pathology,<sup>5</sup> and Biochemistry and Immunology,<sup>7</sup> Institute of Biological Sciences, Federal University of Minas Gerais, Belo Horizonte, Minas Gerais CEP 31270-901, Brazil; Roberts Research Institute<sup>2</sup> and Department of Physiology and Pharmacology<sup>8</sup> and Department of Anatomy and Cell Biology,<sup>9</sup> Schulich School of Medicine & Dentistry, University of Western Ontario, London, Ontario N6A 5K8, Canada; School of Physical Education and Sport<sup>4</sup> and Cardiomyopathy Unit, Heart Institute (InCor),<sup>11</sup> University of São Paulo, São Paulo, São Paulo CEP 05508-900, Brazil; Department of Cell Biology, Duke University Medical Center, Durham, North Carolina 27710<sup>6</sup>; Department of Physics, Institute of Exact Sciences, Federal University of Minas Gerais, Belo Horizonte, Minas Gerais CEP 31270-901, Brazil<sup>10</sup>; and Faculty of Medicine, Federal University of Minas Gerais, Belo Horizonte, Minas Gerais CEP 30130-100, Brazil<sup>12</sup>*

Received 28 July 2009/Returned for modification 3 September 2009/Accepted 8 January 2010

**Overwhelming evidence supports the importance of the sympathetic nervous system in heart failure. In contrast, much less is known about the role of failing cholinergic neurotransmission in cardiac disease. By using a unique genetically modified mouse line with reduced expression of the vesicular acetylcholine transporter (VACHT) and consequently decreased release of acetylcholine, we investigated the consequences of altered cholinergic tone for cardiac function. M-mode echocardiography, hemodynamic experiments, analysis of isolated perfused hearts, and measurements of cardiomyocyte contraction indicated that VACHT mutant mice have decreased left ventricle function associated with altered calcium handling. Gene expression was analyzed by quantitative reverse transcriptase PCR and Western blotting, and the results indicated that VACHT mutant mice have profound cardiac remodeling and reactivation of the fetal gene program. This phenotype was attributable to reduced cholinergic tone, since administration of the cholinesterase inhibitor pyridostigmine for 2 weeks reversed the cardiac phenotype in mutant mice. Our findings provide direct evidence that decreased cholinergic neurotransmission and underlying autonomic imbalance cause plastic alterations that contribute to heart dysfunction.**

The role of sustained cholinergic tone in long-term cardiac function is poorly understood. Cardiac regulation by the parasympathetic nervous system is mediated primarily by acetylcholine (ACh) binding to the M<sub>2</sub> muscarinic ACh receptor (M<sub>2</sub>-AChR) (12). In addition, cholinergic tone also controls sympathetic activity, as preganglionic neurotransmission is cholinergic in the two branches of the autonomic nervous system. Reduced parasympathetic function occurs during aging (11) and has been observed for patients with several disorders that ultimately affect cardiac

function, such as heart failure (15), diabetes (29), and hypertension (13, 50). Moreover, excessive adrenergic activation in association with diminished parasympathetic activity is detrimental in cases of heart failure (35). Recent studies demonstrated that M<sub>2</sub>-AChR knockout (KO) mice exhibit impaired ventricular function and increased susceptibility to cardiac stress, suggesting a protective role of the parasympathetic nervous system in the heart (26). In support of this hypothesis, vagal stimulation has been shown to be of benefit in cases of heart failure (28). While most of these studies focus on possible protective actions of vagal activity and their relation to arrhythmogenesis, the mechanisms associated with the regulation of ventricular contractility by cholinergic neurotransmission are still unclear.

ACh-mediated signaling plays important roles in maintaining synaptic connections during development (5, 9, 32); hence, chronic disturbance of cholinergic tone, as observed in cases of dysautonomia, could contribute to altered myocardial function. Rich cholinergic innervations are found in the sinoatrial node (SAN), the atrial myocardium, the atrioventricular node, and the ventricular conducting system in many species (24).

\* Corresponding author. Mailing address for Silvia Guatimosim: Institute of Biological Sciences, Federal University of Minas Gerais, Av. Antônio Carlos 6627, Belo Horizonte, MG CEP 31270-901, Brazil. Phone: 55 (31) 3409-2952. Fax: 55 (31) 3409-2924. E-mail: guatimosim@icb.ufmg.br. Mailing address for Marco A. M. Prado: Roberts Research Institute, University of Western Ontario, P.O. Box 5015, 100 Perth Drive, London, ON N6A 5K8, Canada. Phone: (519) 663-5777, ext. 36888. Fax: (519) 663-3789. E-mail: mprado@robarts.ca.

† These authors contributed equally to this work.

‡ Supplemental material for this article may be found at <http://mcb.asm.org/>.

<sup>∇</sup> Published ahead of print on 1 February 2010.

Although less abundant, parasympathetic fibers are also found throughout the ventricles, where stimulation of  $M_2$ -AChR by ACh leads to L-type calcium channel inhibition and consequently reduced cardiomyocyte contractility (34).

Genetic disturbance of cholinergic neurotransmission in animal models is complicated, due to the requirement of ACh release to sustain motor function. Thus, the consequences of chronically reduced cholinergic neurotransmission for long-term cardiac function and molecular remodeling have not been studied in detail until now. Given the abundance of acetylcholine receptors, it is likely that genetic disturbance of individual receptors may not reveal all the consequences of decreased cholinergic tone. We have recently generated a mouse model of cholinergic dysfunction (VACHT knockdown, homozygous [VACHT  $KD^{HOM}$ ]) by targeting using homologous recombination for the vesicular ACh transporter (VACHT), a protein responsible for packaging ACh in secretory vesicles (41). VACHT  $KD^{HOM}$  mice have an approximately 70% reduction in the levels of VACHT (41). Here, we used this unique mouse model to investigate whether long-term reduction of cholinergic neurotransmission affects cardiac physiology.

The present studies demonstrate that autonomic imbalance, due to chronic decrease of cholinergic neurotransmission in VACHT mutant mice, is associated with altered gene expression that underlies a heart dysfunction phenotype. Additionally, we show that enhancement of cholinergic activity is beneficial in improving cardiac alterations in VACHT mutant mice. Our findings provide novel insights on mechanisms and compensatory changes found in hearts subjected to prolonged alterations in autonomic regulation. These data support the notion that the cholinergic system is an important pharmacological target in heart failure.

## MATERIALS AND METHODS

**Animal models and drug administration.** VACHT mutant mice (VACHT  $KD^{HOM}$ ) were described previously (41). VACHT mutant mice were generated by targeting the 5' untranslated region of the VACHT gene by homologous recombination in a mixed 129S6/SvEvTac  $\times$  C57BL/6J background and were backcrossed to C57BL/6Uni (from the University of Campinas) for 3 generations (N3), as further backcrossing into the C57BL/6 background caused infertility (data not shown). Heterozygous mice were intercrossed to generate the VACHT mutant and wild-type controls used in these experiments. Wild-type and mutant mice 1, 3, or 6 months old were used in this study for evaluation of cardiac function and myocyte  $Ca^{2+}$  transients. Pyridostigmine (Pyr; Sigma) administration to mice was performed twice daily by intraperitoneal injection for two weeks (1 mg/kg body weight).

VACHT-null mice (VACHT<sup>del/del</sup>), in which the VACHT open reading frame (ORF) was deleted by using Cre/loxP, were described previously (9). VACHT<sup>del/del</sup> mice die shortly after birth due to respiratory failure; therefore, experiments were performed with embryonic day 18.5 (E18.5) embryos. VACHT<sup>wt/del</sup> mice were intercrossed to generate the VACHT-null mice.

Animals were housed in groups of three to five per cage in a temperature-controlled room with 12-h/12-h light/dark cycles in microisolator cages. Food and water were provided *ad libitum*.

Animals were maintained at the Federal University of Minas Gerais (UFMG), Brazil, and at the University of Western Ontario in accordance with NIH guidelines for the care and use of animals. Experiments were performed according to approved animal protocols from the Institutional Animal Care and Use Committee at the UFMG and at the University of Western Ontario.

**Hemodynamic measurements.** Invasive left ventricle (LV) hemodynamic measurements were made using a Millar Mikro-tip pressure transducer (Millar Instruments, Houston, TX) as previously described (20, 33, 51). LV parameters, according to the blood pressure module in Chart analysis software (PowerLab; AD Instruments), were obtained at the baseline and following the administration

of isoproterenol (ISO; 0.02  $\mu$ g or 0.5  $\mu$ g intraperitoneally [i.p.]) as previously described for anesthetized mice (17).

**M-mode echocardiography.** Cardiac function under noninvasive conditions was assessed by two-dimensional guided M-mode echocardiography of halothane-anesthetized mice as previously described (2). Heart rates (HRs) recorded under this condition were  $541.5 \pm 21.4$  beats per min (bpm) for the wild-type (WT) mice (8 mice),  $520.2 \pm 25.2$  bpm for the VACHT  $KD^{HOM}$  mice (5 mice), and  $549.0 \pm 23.4$  bpm for the VACHT  $KD^{HOM}$  mice with Pyr (5 mice).

**Electrocardiography.** A dorsally mounted radio frequency transmitter and wire leads (lead II configuration) were implanted subcutaneously under anesthesia. Chronic electrocardiogram (ECG) recordings from conscious mice were acquired with the Data Sciences International telemetry system (Transoma Medical, St. Paul, MN) as previously described (33). ECG recordings were initiated following a minimum of 7 days postimplantation. HR and HR variability (HRV) parameters were obtained and analyzed under basal (saline), atropine (1 mg/kg, i.p.), propranolol (1 mg/kg, i.p.), or atropine-plus-propranolol conditions by using the Dataquest A.R.T. software (Transoma Medical). The analysis for both HR and HRV was performed 15 min following administration of drugs.

**Cardiomyocyte isolation and  $Ca^{2+}$  recordings.** Adult ventricular myocytes were freshly isolated and stored in Dulbecco's modified Eagle's medium (DMEM; Sigma) until they were used (within 6 h) as previously described (21). Intracellular  $Ca^{2+}$  imaging experiments were performed with Fluo-4 AM (10  $\mu$ M; Invitrogen, Eugene, OR)-loaded cardiomyocytes for 25 min, and these were subsequently washed with an extracellular solution that contained 1.8 mmol/liter  $Ca^{2+}$  to remove the excess dye. Cells were electrically stimulated at 1 Hz to produce steady-state conditions. The confocal line-scan imaging was performed with a Zeiss LSM 510META confocal microscope. The amplitude of the  $Ca^{2+}$  transient evoked by the application of a  $Ca^{2+}$ - and  $Na^{+}$ -free solution containing 10 mM caffeine was used as an indicator of the SR  $Ca^{2+}$  load (36). Cells were subjected to a series of preconditioning pulses (1 Hz) before caffeine was applied.  $Ca^{2+}$  spark frequencies in resting ventricular myocytes were recorded. Digital image processing was performed by using custom-devised routines created with the IDL programming language (Research Systems, Boulder, CO). The  $Ca^{2+}$  level was reported as  $F/F_0$  (or as  $\Delta F/F_0$ ), where  $F_0$  is the resting  $Ca^{2+}$  fluorescence.

**Langendorff preparation-perfused hearts.** Briefly, once removed from the animal, the heart was perfused with a Krebs-Ringer solution, which was delivered at 37°C with continuous gassing with 5%  $CO_2$  to yield a physiological pH of 7.4. Hearts were perfused with this solution for 50 min as previously described for mice and rats (6, 14).

**Histological assessment of cardiac fibrosis.** In both WT and VACHT  $KD^{HOM}$  groups, the fibrotic area in the LV and interventricular septum (IS) was evaluated by Masson's trichrome staining. Whole hearts were harvested, fixed in 10% formaldehyde, embedded in paraffin, and cut into sections 6  $\mu$ m thick. Tissue sections were collected from atrial and ventricular regions, mounted on slides, and postfixed in Bouin's solution. After a series of xylene and alcohol washes were performed, slides were stained with Weigert's hematoxylin and Masson's trichrome staining solutions. Then, slides were subjected to increased concentrations of alcohol and xylene and mounted with Entellan.

**Quantitative PCR.** For RNA purifications, tissues were grounded in a potter with a pestle with liquid nitrogen, and total RNA was extracted using Trizol. For quantitative PCR (qPCR), total RNA was treated with DNase I (Ambion, Austin, TX), and first-strand cDNA was synthesized using the High-Capacity cDNA transcription kit (Applied Biosystems, CA) according to the manufacturer's instructions. After reverse transcription, the cDNA was subjected to qPCR on a 7500 real-time PCR system (Applied Biosystems, CA) by using Power SYBR green PCR master mix (Applied Biosystems, CA). Briefly, amplification was carried out in a total volume of 20  $\mu$ l containing 0.5  $\mu$ M each primer, 10  $\mu$ l of Power SYBR green master mix (2 $\times$ ), and 1  $\mu$ l of cDNA. The PCRs were cycled 45 times after initial denaturation (95°C, 2 min) with the following parameters: 95°C for 15 s, annealing at 60°C for 30 s, and extension at 72°C for 30 s. For each experiment, a nontemplate reaction was included as a negative control. In addition, the absence of DNA contaminants was assessed in reverse transcriptase-negative samples. Melting curve analysis of amplification products was performed by cooling the samples to 60°C and then increasing the temperature to 95°C at 0.1°C/s. The specificity of the PCRs was also confirmed by size verification of the amplicons in acrylamide gel. Relative quantification of gene expression was done with the  $2^{-\Delta\Delta CT}$  method, using the  $\beta$ -actin gene expression to normalize the data. Sequences of primers used are available upon request.

**Immunofluorescence.** Images were acquired with an Axiovert 200 M microscope coupled with the ApoTome system or a Leica SP5 confocal microscope to obtain optical sections of the tissue. Objectives used were 20 $\times$  dry, 40 $\times$  water immersion (1.2 numerical aperture [NA]), and 63 $\times$  oil immersion (1.4 NA). Adult VACHT  $KD^{HOM}$  and WT mice were anesthetized with ketamine and

xylazine (70 and 10 mg/kg i.p., respectively) and transcardially perfused with ice-cold phosphate-buffered saline (PBS), pH 7.4, for 10 min, followed by an ice-cold solution of methanol containing 20% dimethyl sulfoxide (DMSO) for 10 min. Immunofluorescence was performed as previously described (10). Slices were incubated for 15 to 18 h with primary antibodies anti-VACHT (rabbit polyclonal, 1:250; Sigma Chemical Co., São Paulo, Brazil) and CHT1 (rabbit polyclonal, 1:250; kindly provided by R. Jane Rylett, University of Western Ontario, London, Ontario, Canada).

Immunofluorescence of adult ventricular cardiomyocytes was performed on cells fixed in 4% paraformaldehyde (PFA) and permeabilized with 0.5% saponin. Anti- $\alpha$ -actinin antibody (Sigma) was used at a dilution of 1:200. Secondary antibody-conjugated to Alexa Fluor 488 or 543 (Molecular Probes) was used at a dilution of 1:1,000, and nuclear staining was performed using DAPI (4',6-diamidino-2-phenylindole) in a dilution of 1:1,000. Cardiomyocyte cellular area in  $\alpha$ -actinin-stained cells was measured.

**Cardiomyocyte morphometry.** The mice were anesthetized with 10% ketamine–2% xylazine (4:3, 0.1 ml/100 g, i.p.), and heartbeat was stopped in diastole by using 10% KCl (intravenous [i.v.]). Hearts were placed in 4% Bouin's fixative for 24 h at room temperature. The tissues were dehydrated by sequential washes with 70, 80, 90, and 100% ethanol and embedded in paraffin. Transversal sections (5  $\mu$ m) were cut starting from base area of the heart at intervals of 40  $\mu$ m and stained with hematoxylin-eosin for cell morphometry. Tissue sections (2 from each animal) were examined with a light microscope (BX 41; Olympus) at  $\times$ 400 magnification, photographed (Q Color 3; Olympus), and analyzed with ImageJ software. Only digitized images of cardiomyocytes cut longitudinally with nuclei and cellular limits visible were used for analysis (an average of 40 cardiomyocytes for each animal). The diameter of each myocyte was measured across the region corresponding to the nucleus.

**Whole-heart morphometry.** Transversal heart sections (5  $\mu$ m) were cut starting from base area of the heart at intervals of 40  $\mu$ m and stained with hematoxylin-eosin. The area of cardiac mass was obtained by subtracting the left and right ventricle chamber areas from the total area of the heart and expressed as a percentage of the total area. Images with  $\times$ 20 magnification were captured using a Q Color 3 camera (Olympus) to measure ventricular and total tissue areas.

**Whole-cell patch clamp and action potential recordings.** An EPC-9.2 instrument (HEKA Electronics) was used to patch clamp single ventricular cardiomyocytes in whole-cell voltage and current clamp configurations, using specific protocols according to the ionic conductance evaluated (8, 36, 42). Measurements started 5 min after breaking into the cell in order to attain equilibrium between the pipette solution and the cell cytoplasm. For action potential (AP) recordings, the pipette solution consisted of 130 mmol/liter K-aspartate, 20 mmol/liter KCl, 10 mmol/liter HEPES, 2 mmol/liter MgCl<sub>2</sub>, 5 mmol/liter NaCl, and 5 mmol/liter EGTA (set to pH 7.2 with KOH). Modified Tyrode used as bath solution contained 140 mmol/liter NaCl, 5.4 mmol/liter KCl, 1 mmol/liter MgCl<sub>2</sub>, 1.8 mmol/liter CaCl<sub>2</sub>, 10 mmol/liter HEPES, and 10 mmol/liter glucose (set at pH 7.4). Current injections triggered action potentials at a constant rate (1 Hz).

For L-type Ca<sup>2+</sup> current (I<sub>CaL</sub>) recordings, the pipette solution contained 120 mM CsCl, 20 mM tetraethylammonium chloride (TEACl), 5 mM NaCl, 10 mM HEPES, 5 mM EGTA (set to pH 7.2 with CsOH). The bath solution was modified Tyrode solution. I<sub>Ca</sub> was elicited by depolarization steps from –40 to 50 mV for 300 ms from a holding potential of –80 mV at a frequency of 0.1 Hz and sample frequency of 10 kHz. To inactivate Na<sup>+</sup> current (I<sub>Na</sub>), we used a prepulse from –80 to –40 mV with a duration of 50 ms.  $\beta$ -Adrenergic stimulation of cells was produced by the addition of 100 nmol/liter isoproterenol to modified Tyrode solution for 3 min. All experiments were carried out at room temperature (23 to 26°C).

**Western blotting.** Forty to 60  $\mu$ g of protein was separated by SDS-PAGE. Antibodies used were anti-SERCA2 and antiphospholamban (anti-PLN) (ABR), anti-phospho-PLN (Ser-16) (Upstate), anti-phospho-PLN (Thr-17) (Badrilla), anti-troponin I (TnI) and anti-phospho-TnI (Cell Signaling), and anti- $\alpha$ -tubulin (Sigma Chemical Co.). Immunodetection was carried out using enhanced chemiluminescence (Amersham Biosciences). Protein levels were expressed as ratios of optical densities.  $\alpha$ -Tubulin was used as a control for any variations in protein loading.

**Statistical analysis.** All data are expressed as means  $\pm$  standard errors of the means (SEM), and the numbers of cells or experiments (*n*) are shown. Significant differences between groups were determined with Student's *t* test or an analysis of variance (ANOVA) followed by the Bonferroni post hoc test. *P* values of <0.05 were considered to be statistically significant.

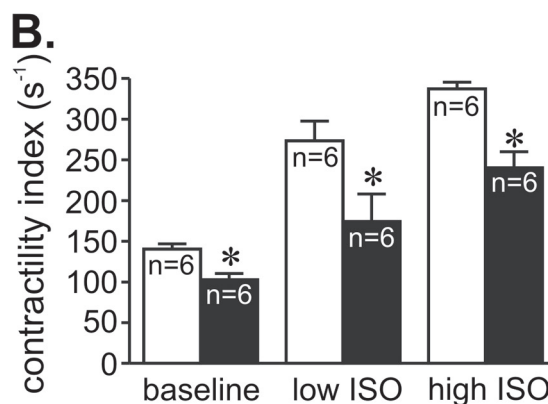
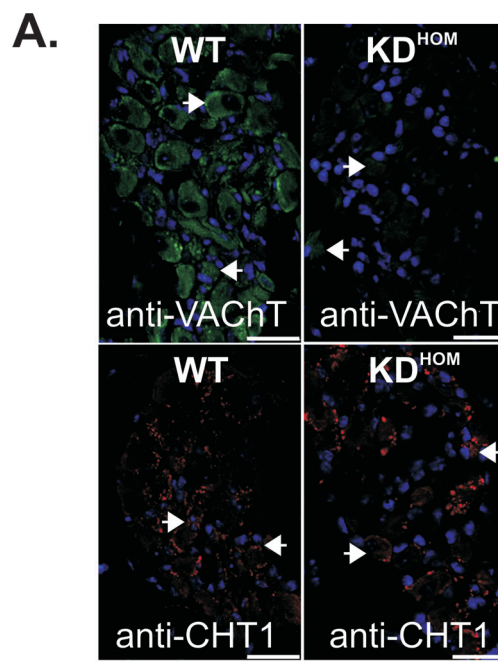


FIG. 1. VACHT mutant mice present heart failure. (A) VACHT and CHT1 immunoreactivity in neurons of adult WT and VACHT KD<sup>HOM</sup> mouse intracardiac ganglia. Note the reduction in immunofluorescence for VACHT. There was no decrease in immunoreactivity in nodal ganglia of VACHT KD<sup>HOM</sup> stained with an antibody against the high-affinity choline transporter (CHT1). Blue labeling corresponds to nuclei stained with DAPI that seem to predominantly label glial cells. Arrowheads indicate some of the neuronal cell bodies in the ganglia. Bar = 20  $\mu$ m. (B) Left ventricle function (as assessed by contractility index) in VACHT KD<sup>HOM</sup> mice (black bars) and WT mice (white bars). VACHT mutant mouse hearts had decreased contractility indexes and lower absolute responses to ISO. *n*, number of mice; \*, *P* value of <0.05 in comparison with the WT.

## RESULTS

**Decreased cholinergic neurotransmission in VACHT KD<sup>HOM</sup> mice causes heart failure.** VACHT KD<sup>HOM</sup> mice have previously been shown to have reduced VACHT expression and altered ACh release (41; R. F. Lima, V. F. Prado, M. A. Prado, and C. Kushmerick, submitted for publication). In agreement with these previous observations, hearts from 3-month-old VACHT KD<sup>HOM</sup> mice had decreased VACHT immunoreactivity in intracardiac ganglia (Fig. 1A; arrowheads indicate some of the

TABLE 1. Hemodynamic parameters for WT and VACHT KD<sup>HOM</sup> mice under baseline and isoproterenol stimulation conditions<sup>a</sup>

Parameter	Baseline <sup>b</sup>		Isoproterenol <sup>b</sup>	
	WT	VACHT KD <sup>HOM</sup>	WT	VACHT KD <sup>HOM</sup>
HR (bpm)	277 ± 26	240 ± 15	621 ± 22	509 ± 43*
LVSP (mm Hg)	104.0 ± 2.4	86.2 ± 6.0*	111.8 ± 10.9	90.7 ± 4.4
LVEDP (mm Hg)	8.3 ± 1.7	11.8 ± 2.4	1.2 ± 1.2	7.5 ± 2.0*
+dP/dt <sub>max</sub> (mm Hg/s)	7,245 ± 388	4,640 ± 573*	16,615 ± 866	10,798 ± 1,295*
-dP/dt <sub>min</sub> (mm Hg/s)	6,739 ± 478	4,591 ± 637*	9,163 ± 436	6,448 ± 375*

<sup>a</sup> HR, heart rate; LVSP, left ventricle systolic pressure; LVEDP, left ventricle end diastolic pressure; +dP/dt<sub>max</sub>, maximum first derivative of the change in left ventricle pressure; -dP/dt<sub>min</sub>, minimum first derivative of the change in left ventricle pressure; \*, P value of <0.05 in comparison to the wild-type value.

<sup>b</sup> Values are means ± SEM (n = 6).

neuronal cell bodies) compared to the WT. In contrast, there was no decrease in immunoreactivity in VACHT KD<sup>HOM</sup> mouse nodal ganglia stained with an antibody against the high-affinity choline transporter (CHT1). These results confirm previous assessments of VACHT and CHT1 expression in VACHT KD<sup>HOM</sup> mice (10, 41). We have shown previously that a constitutive lack of cholinergic tone affects skeletal muscle function and ability to perform exercise in VACHT KD<sup>HOM</sup> mice (41). Moreover, the lack of VACHT in KO mice affects skeletal muscle development (9). In order to determine if the constitutive decrease in cholinergic tone could affect cardiomyocytes and, hence, heart physiology, we performed invasive hemodynamic assessments on anesthetized mice. These experiments revealed a reduced contractility index (maximum first derivative of the change in left ventricle pressure [dP/dt] divided by the LV pressure at the time of maximum dP/dt) in the hearts of 3-month-old VACHT KD<sup>HOM</sup> mice compared to that of WT controls (Fig. 1B). Peak left ventricle systolic pressure and the maximum rates of LV pressure rise and fall (peak +dP/dt and -dP/dt, respectively) were also significantly lower in VACHT mutants than in WT mice under baseline conditions (Table 1). Furthermore, an attenuated response to ISO by VACHT mutants was evident (Fig. 1B and Table 1). Although the absolute effect shows a decrease in the ISO-mediated response by VACHT mutants, the relative increases in contractility index were not significantly different between WT and VACHT mutants. In order to investigate the progression of cardiac dysfunction in VACHT mutants, we have also performed hemodynamic assessments of 1-month-old VACHT mutant mice. In contrast to 3-month-old mice according to the obtained data, younger mice did not show differences in the contractility index under either baseline (WT, 134 ± 22 s<sup>-1</sup> [n = 4]; VACHT KD<sup>HOM</sup>, 135 ± 6 s<sup>-1</sup> [n = 5]) or maximal ISO stimulation (WT, 251 ± 17 s<sup>-1</sup> [n = 4]; VACHT KD<sup>HOM</sup>, 303 ± 24 s<sup>-1</sup> [n = 5]) conditions. Therefore, all subsequent experiments were performed with 3-month-old mice.

To ascertain the extension of cardiac dysfunction in 3-month-old VACHT KD<sup>HOM</sup> mice “*in vivo*,” we performed two-dimensional M-mode echocardiography. As shown in Fig. 2A, VACHT KD<sup>HOM</sup> mice displayed reduced left ventricle fractional shortening, consistent with the heart dysfunction illustrated in Fig. 1B. To further confirm that the decreased baseline fractional shortening was indeed the result of altered cholinergic function *in vivo*, we treated VACHT KD<sup>HOM</sup> mice for 2 weeks with a cholinesterase inhibitor, with the rationale that pharmacological restoration of ACh at synapses might rescue the phenotype and improve cardiac function in mutant mice. Administration of pyridostigmine for 2 weeks signifi-

cantly increased fractional shortening of VACHT KD<sup>HOM</sup> mice toward control levels (Fig. 2A). To further assess directly the heart dysfunction in VACHT KD<sup>HOM</sup> mice without the complication of extensive regulation by the autonomic nervous system, we used the Langerdorff isolated heart preparation. In agreement with the results obtained with echocardiography studies, isolated hearts from VACHT KD<sup>HOM</sup> mice had significantly decreased systolic tension compared to WT hearts (Fig. 2B). Pyridostigmine treatment of animals for 2 weeks also reversed the decreased systolic tension in isolated VACHT KD<sup>HOM</sup> hearts measured *in vitro*. Similarly, a contractile dysfunction was observed in isolated adult ventricular cardiomyocytes from VACHT KD<sup>HOM</sup> mice, which demonstrated reduced fractional shortening compared to cardiomyocytes from WT mice (see Fig. S1A in the supplemental material).

In agreement with the data showing heart dysfunction in VACHT KD<sup>HOM</sup> mice, transcripts encoding atrial natriuretic factor (ANF), β-myosin heavy chain (β-MHC), and B-type natriuretic peptide (BNP), markers of cardiac stress, were also upregulated in cardiomyocytes from VACHT mutants. These changes were reversed by pyridostigmine treatment, suggesting that they are triggered by reduced cholinergic neurotransmission (Fig. 2C).

One possible reason for the alteration in cardiac function in VACHT KD<sup>HOM</sup> mice might be related to an increase in blood pressure or HR. Contrary to this prediction, decreased cholinergic tone in VACHT KD<sup>HOM</sup> mice was associated with reduced arterial pressure (see Fig. S1B in the supplemental material), with no significant alteration in basal HR using the tail-cuff system (715 ± 9 bpm for WT mice [n = 17] versus 698 ± 10 bpm for VACHT KD<sup>HOM</sup> mice [n = 16]). Similarly, no significant differences were observed in HR as determined by telemetry comparing WT and VACHT KD<sup>HOM</sup> mice (530 ± 45 bpm for WT mice [n = 3] versus 615 ± 26 bpm for KD<sup>HOM</sup> mice [n = 3]; P = 0.18). Additionally, HRs of VACHT KD<sup>HOM</sup> and WT mice under anesthesia were not significantly different (Table 1), and this contrasted with significantly reduced HRs recorded from *ex vivo* beating hearts from VACHT KD<sup>HOM</sup> mice compared to those from WT controls (Fig. 2D).

Importantly, heart dysfunction observed in VACHT mutant mice was not linked to cardiac fibrosis (see Fig. S1C in the supplemental material) and hypertrophy. Instead, cardiac mass (Table 2), morphometric analyses of cross-sectional area (see Fig. S1D in the supplemental material), and cellular area measurements (1,992.0 ± 78.5 μm<sup>2</sup> cell area in WT mice [29 cells] versus 1,318.0 ± 60.4 μm<sup>2</sup> in VACHT KD<sup>HOM</sup> mice [40 cells]; P < 0.05) indicated that both the heart and cardiomyocytes

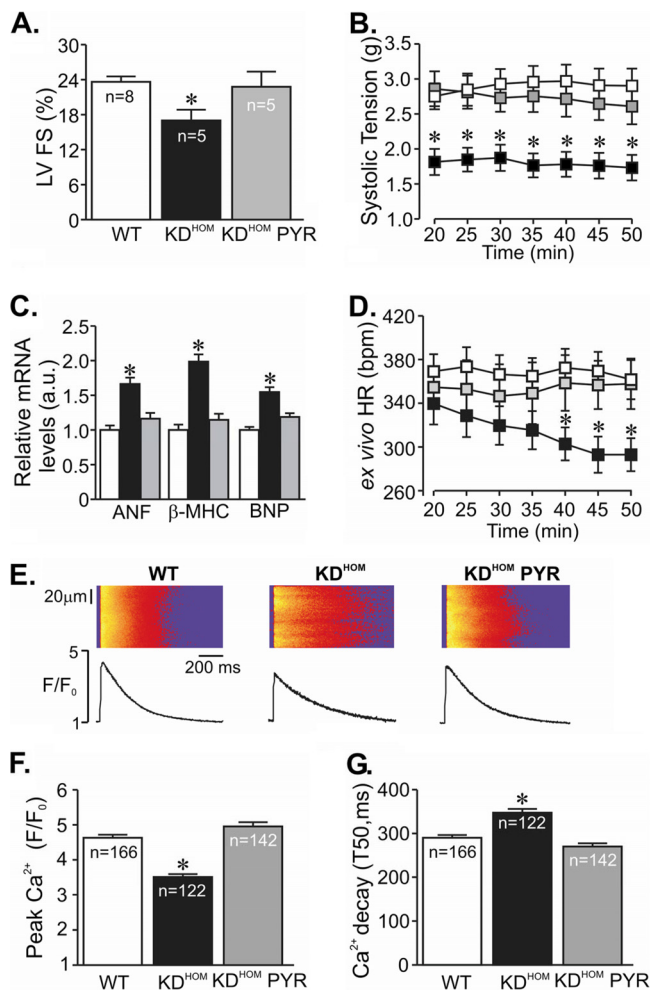


FIG. 2. Pyridostigmine treatment prevented cardiac dysfunction in VACHT  $KD^{HOM}$  mice. (A) Echocardiography analysis of left ventricle fractional shortening (FS) in VACHT mutant mice (black bars) and WT mice (white bars). Note the significant improvement in left ventricle performance after pyridostigmine treatment (gray bars). n, number of mice. (B) Time course of systolic tension in isolated perfused hearts from WT (white squares; 15 hearts) and VACHT  $KD^{HOM}$  (black squares; 16 hearts) mice. Pyridostigmine treatment improved systolic tension of hearts from mutant mice (gray squares; 4 hearts). (C) Gene expression of stress cardiac markers in cardiomyocytes from VACHT  $KD^{HOM}$  mice and WT mice. The bar graph shows data from at least 5 independent experiments. a.u., arbitrary units. (D) The HR measured in *ex vivo* beating hearts from VACHT  $KD^{HOM}$  mutants (black squares) was lower than that of WT hearts (white squares) after 40 min of perfusion. Pyridostigmine treatment for 2 weeks (gray squares) prevented the observed changes in HR. (E) (Top) Representative confocal images of electrically stimulated intracellular  $Ca^{2+}$  transient recordings in ventricular myocytes. (Bottom)  $Ca^{2+}$  transient line-scan profile. (F) Significant reduction in peak  $Ca^{2+}$  transient amplitude observed in freshly isolated adult VACHT  $KD^{HOM}$  ventricular cardiomyocytes compared to the amplitude for WT mice. Pyridostigmine treatment significantly prevented intracellular  $Ca^{2+}$  dysfunction in VACHT  $KD^{HOM}$  mice. n, number of ventricular cardiomyocytes analyzed. (G)  $Ca^{2+}$  transient kinetics of decay in VACHT  $KD^{HOM}$  cardiomyocytes and WT mice. Note that the observed changes in myocytes from VACHT  $KD^{HOM}$  mice can be prevented by 2 weeks of pyridostigmine treatment. \*, *P* value of  $<0.05$  in comparison with WT and  $KD^{HOM}$  PYR mice. T50, time from peak  $Ca^{2+}$  transient to 50% decay.

TABLE 2. Phenotypic parameters for WT and VACHT  $KD^{HOM}$  mice<sup>a</sup>

Parameter	WT (n = 23) <sup>b</sup>	$KD^{HOM}$ (n = 26) <sup>b</sup>
BW (g)	24.26 ± 0.51	22.53 ± 0.36
HW (mg)	193.50 ± 4.82	177.30 ± 4.36
HW/TL ratio (mg/mm)	8.80 ± 0.25	7.96 ± 0.16

<sup>a</sup> BW, body weight; HW, heart weight; HW/TL, heart weight/tibia length ratio.

<sup>b</sup> Values are means ± SEM. The *P* values were  $<0.05$  for all conditions in comparisons of the values for the wild-type and VACHT  $KD^{HOM}$  mice.

from VACHT mutant were significantly smaller than those of the WT mice at 3 months. However, it is possible that hypertrophy may develop or progress in mutant hearts as a result of depressed cholinergic drive with age. In fact, hearts from 6-month-old mutants presented more pronounced changes in cardiac structure characterized by concentric hypertrophy compared to age-matched controls (see Fig. S1E and F in the supplemental material). Taken together, these data suggest that VACHT mutants have progressive changes in cardiac mass. Herein, we focused our experiments on 3-month-old mice.

Altered  $Ca^{2+}$  handling can influence cardiomyocyte physiology and changes in intracellular  $Ca^{2+}$  are a major feature in heart failure and myocyte pathology (3, 4). To determine if the heart dysfunction detected in VACHT  $KD^{HOM}$  mice is related to changes in  $Ca^{2+}$  handling, we examined intracellular  $Ca^{2+}$  in freshly isolated Fluo-4 AM-loaded ventricular myocytes from 3-month-old VACHT  $KD^{HOM}$  and WT mice. Figure 2E displays typical line-scan fluorescence images recorded from electrically stimulated ventricular myocytes. VACHT  $KD^{HOM}$  cardiomyocytes developed significantly smaller and slower intracellular  $Ca^{2+}$  transients than WT cells. The amplitude of the  $Ca^{2+}$  transient was significantly reduced in VACHT  $KD^{HOM}$  cardiomyocytes (Fig. 2F), and the kinetics of  $Ca^{2+}$  decay were significantly slower (Fig. 2G). These changes are closely related to the alteration in cholinergic tone in VACHT mutant mice, as  $Ca^{2+}$  handling is restored to normal levels in cells obtained from pyridostigmine-treated VACHT  $KD^{HOM}$  mice. Hence, changes in intracellular calcium handling parallel alterations in cardiac function due to reduced cholinergic tone. Collectively, these results suggest a correlation between decreased cholinergic tone and heart dysfunction that can be recovered by cholinesterase inhibitor treatment.

**Cardiomyocyte remodeling in VACHT  $KD^{HOM}$  mice.** To investigate the cellular basis of the abnormal intracellular  $Ca^{2+}$  transient of failing VACHT  $KD^{HOM}$  cardiomyocytes, electrical activity and expression levels of  $Ca^{2+}$  handling proteins were assessed by electrophysiology and Western blotting techniques, respectively. First, we investigated whether possible changes in  $I_{Ca}$  may play a role in the  $Ca^{2+}$  signaling dysfunction observed in VACHT  $KD^{HOM}$  cardiac cells. Figure 3A shows sample  $I_{Ca}$  recordings. Virtually no difference between macroscopic  $I_{Ca}$  values recorded in VACHT  $KD^{HOM}$  and WT cells was observed (at 0 mV,  $-8.10 \pm 0.44$  pA/pF in 12 WT cardiomyocytes versus  $-7.98 \pm 0.39$  pA/pF in 20 VACHT  $KD^{HOM}$  cardiomyocytes) (Fig. 3B), suggesting that under basal conditions,  $Ca^{2+}$  currents of the two genotypes were identical. Activation of  $\beta_1$ -adrenergic receptor increases  $I_{Ca}$ , and this is in part responsible for the adrenergic regulation of myocytes. Although we

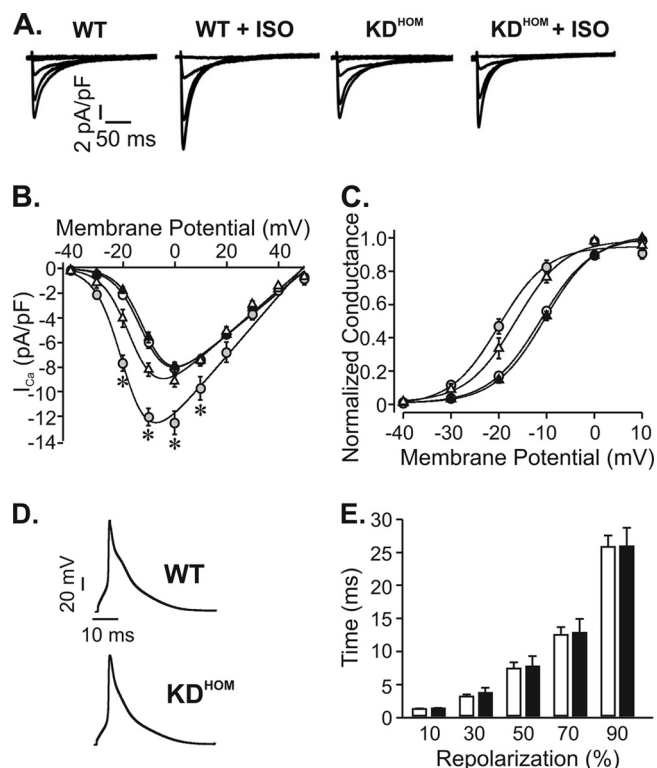


FIG. 3. Electrical properties of VAcHT KD<sup>HOM</sup> cardiomyocytes. (A) Sample I<sub>Ca</sub> currents recorded from depolarizations from -40 mV to 0 mV. ISO (100 nmol/liter) significantly increased the magnitude of I<sub>Ca</sub> in WT cells but not in VAcHT KD<sup>HOM</sup> ventricular myocytes. (B) Average I-V relationships for I<sub>Ca</sub> current density recorded from WT mice (open circles), WT mice with ISO (gray circles), VAcHT KD<sup>HOM</sup> mice (black triangles), and VAcHT KD<sup>HOM</sup> mice with ISO (open triangles). (C) Steady-state activation curves. (D) Sample action potential recordings from WT and VAcHT KD<sup>HOM</sup> ventricular cardiomyocytes. (E) Action potential durations at 10, 30, 50, 70, and 90% repolarization. Fifteen cells from each experimental group were used. \*, P value of <0.05 in comparison with WT mice.

have not observed a significant change in ISO-mediated response *in vivo*, it is possible that at the cellular level, β-adrenergic responses are altered; therefore, we next evaluated I<sub>Ca</sub> levels in myocytes exposed to ISO (100 nM). Figure 3A to C show that the I<sub>Ca</sub> increase induced by ISO was much less prominent in VAcHT KD<sup>HOM</sup> ventricular myocytes.

Alterations in action potential profile may also contribute to dampening Ca<sup>2+</sup> cycling in ventricular cells. To investigate this possible contribution, we recorded action potentials in ventricular myocytes from WT and VAcHT KD<sup>HOM</sup> mice. No change between the action potential profiles of these cells was observed (Fig. 3D and E), indicating that electrical changes were not contributing to the Ca<sup>2+</sup> signaling dysfunction observed in response to decreased cholinergic tone.

The slow decline of the Ca<sup>2+</sup> transient in VAcHT KD<sup>HOM</sup> cardiomyocytes is consistent with the decreased expression of the sarcoplasmic reticulum (SR) Ca<sup>2+</sup> pump (SERCA2); therefore, we examined SERCA2 levels in these hearts. A significant reduction in SERCA2 expression levels was observed in VAcHT KD<sup>HOM</sup> hearts (Fig. 4A) compared to WT controls. In cardiac cells, PLN is the primary determinant of

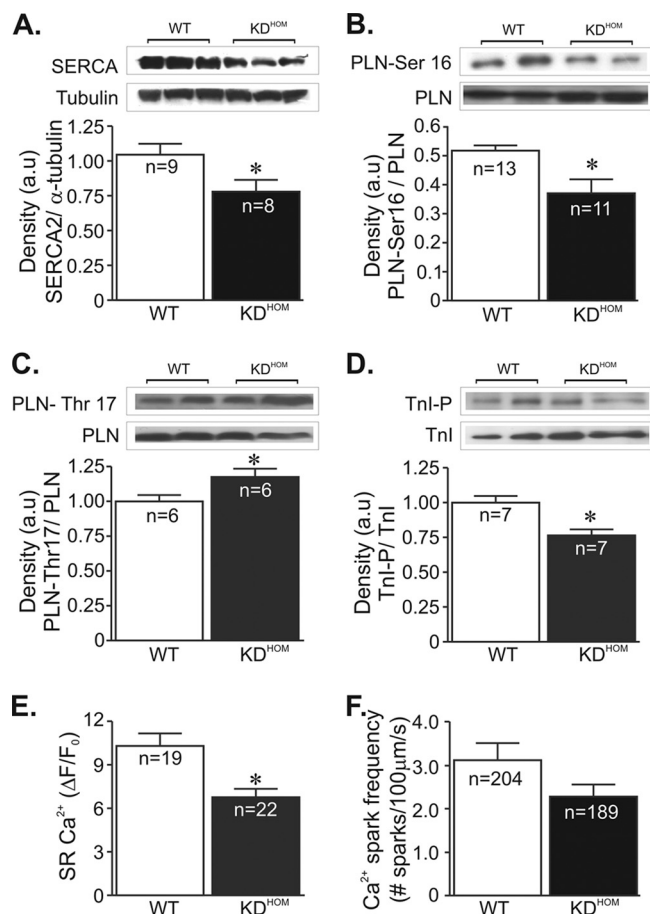


FIG. 4. Ca<sup>2+</sup> signaling components in VAcHT KD<sup>HOM</sup> hearts. In panels A to D, the top image is a representative Western blot and the bottom shows an average densitometry graph (n, number of heart samples analyzed). (A) SERCA2 levels in VAcHT KD<sup>HOM</sup> hearts were observed to be significantly reduced compared to levels in WT hearts. Phosphorylated-PLN levels at the protein kinase A (PKA)-dependent site (Ser-16) were lower in VAcHT mutant hearts (B), while phospho-Thr-17-PLN levels were increased in these hearts (C). (D) Phospho-Ser-23/24-troponin I levels were decreased in VAcHT mutant hearts relative to WT hearts. Tubulin expression levels were used as a loading control. (E) The SR Ca<sup>2+</sup> content in ventricular cardiomyocytes from VAcHT mutants was significantly reduced compared to that in WT cells. n, number of cells. (F) Ca<sup>2+</sup> spark frequency showed a tendency to be lower in VAcHT KD<sup>HOM</sup> cardiomyocytes than in WT mice, but the difference was not statistically different. n, number of cells. \*, P < 0.05.

SERCA2 function. Therefore, we also investigated if there may be a change in PLN activity in VAcHT KD<sup>HOM</sup> hearts by examining PLN expression/phosphorylation levels in these hearts. PLN expression was higher in VAcHT KD<sup>HOM</sup> hearts (data not shown); however, as shown in Fig. 4B, phosphorylated-PLN levels at Ser-16, a key determinant of SERCA2 activity, were significantly reduced in these hearts. We have also assessed PLN phosphorylation levels at the CaMKII site (Thr-17). Phospho-Thr-17-PLN levels in VAcHT KD<sup>HOM</sup> hearts were significantly increased compared to those in WT hearts (Fig. 4C). Another important aspect of cardiac cells is the sensitivity of the myofilaments to Ca<sup>2+</sup>. Since TnI phosphorylation desensitizes the myofilament to Ca<sup>2+</sup>, we next

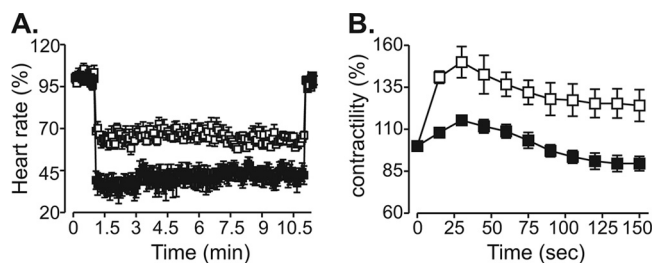


FIG. 5. VACHT KD<sup>HOM</sup> hearts present an altered GPCR response. (A) Percent decrease in beating frequency for WT (white squares;  $n = 4$ ) and VACHT KD<sup>HOM</sup> (black squares;  $n = 4$ ) hearts in response to 13  $\mu\text{mol/liter}$  ACh. (B) Time course of mean percent force increase in WT ( $n = 5$ ) and VACHT KD<sup>HOM</sup> ( $n = 5$ ) perfused hearts in response to 10  $\mu\text{mol/liter}$  ISO.

assessed TnI phosphorylation levels in cardiac samples. As shown in Fig. 4D, phospho-Ser-23/24-troponin I levels were significantly decreased in VACHT KD<sup>HOM</sup> hearts compared to WT hearts.

Since the SERCA2/PLN ratio is altered in the VACHT KD<sup>HOM</sup> hearts, we next examined the possibility that this alteration may lead to a reduction of  $\text{Ca}^{2+}$  in the SR. Figure 4E shows a significant reduction in SR  $\text{Ca}^{2+}$  content in VACHT KD<sup>HOM</sup> cardiomyocytes. Furthermore,  $\text{Ca}^{2+}$  sparks were less frequent in VACHT KD<sup>HOM</sup> cardiomyocytes than in WT mice (Fig. 4F), although the data just failed to reach statistical significance.

**VACHT KD<sup>HOM</sup> mice show altered autonomic control of heart rate and G-protein-coupled receptor (GPCR) function.** A chronic decrease in cholinergic tone in VACHT KD<sup>HOM</sup> mice appears to cause molecular cardiac remodeling with alterations in expression of genes related to cardiac stress,  $\text{Ca}^{2+}$  handling, and muscle contractility. Moreover, data from recordings of calcium currents suggested that  $\beta_1$ -adrenergic receptor responses are altered in VACHT KD<sup>HOM</sup> cardiomyocytes. To determine if decreased cholinergic tone, caused by reduced release of ACh in VACHT mutant mice, affected the responses to muscarinic and adrenergic activation, we treated Langendorff preparation-perfused hearts with ACh or ISO. As shown in Fig. 5A, hearts from VACHT KD<sup>HOM</sup> mice were much more sensitive to ACh (13  $\mu\text{mol/liter}$ ) than hearts from WT mice, and they showed enhanced bradycardia in response to this neurotransmitter. In contrast, the contractility response of *ex vivo* beating hearts from VACHT KD<sup>HOM</sup> mice to ISO (10  $\mu\text{mol/liter}$ ) was significantly attenuated (Fig. 5B), providing additional evidence of altered adrenergic response in mutant hearts.

To examine the possibility of autonomic imbalance in 3-month-old VACHT KD<sup>HOM</sup> mice *in vivo*, we assessed the effects of muscarinic and adrenergic receptor blockades on HR and HR variability parameters. Administration of atropine did not significantly increase HRs in either WT ( $\Delta\text{HR}$ ,  $56 \pm 27$  bpm) or VACHT KD<sup>HOM</sup> ( $\Delta\text{HR}$ ,  $65 \pm 28$  bpm) mice, whereas propranolol administration significantly reduced the HR in VACHT KD<sup>HOM</sup> mice ( $\Delta\text{HR}$ ,  $-115 \pm 27$  bpm;  $P < 0.05$ ) but not in WT mice ( $\Delta\text{HR}$ ,  $-78 \pm 40$  bpm). Interestingly, the coadministration of atropine and propranolol resulted in a significant reduction of HR in VACHT KD<sup>HOM</sup> mice ( $\Delta\text{HR}$ ,  $-87 \pm 13$  bpm;  $P < 0.05$ ) but not in WT mice ( $\Delta\text{HR}$ ,  $-11 \pm 4$

bpm). These results would suggest that HR in VACHT KD<sup>HOM</sup> mice is under increased sympathetic control relative to HR in WT mice. To further investigate autonomic imbalance, we examined HRV parameters. Under baseline conditions, no significant differences in very low frequency (VLF) and low frequency (LF) power spectrum of HRV between WT and VACHT KD<sup>HOM</sup> mice were observed (data not shown). However, high-frequency (HF) power was significantly increased in VACHT KD<sup>HOM</sup> mice (HF,  $3.66 \pm 0.18$   $\text{ms}^2$ ;  $n = 3$ ) compared to WT mice (HF,  $1.98 \pm 0.42$   $\text{ms}^2$ ;  $n = 3$ ), which resulted in a significant difference between the LF/HF ratios of the genotypes ( $4.2 \pm 0.6$  for KD<sup>HOM</sup> mice [ $n = 3$ ] versus  $6.6 \pm 0.5$  for WT mice [ $n = 3$ ];  $P = 0.04$ ). Atropine administration significantly reduced the LF/HF ratio in both WT ( $1.2 \pm 0.5$ ;  $n = 3$ ) and VACHT KD<sup>HOM</sup> ( $1.6 \pm 0.8$ ;  $n = 3$ ) mice, and these values were not different between genotypes. Interestingly, propranolol treatment did not significantly alter the LF/HF ratios relative to the baseline LF/HF ratios for either WT or VACHT KD<sup>HOM</sup> mice (data not shown). Lastly, the coadministration of atropine and propranolol significantly reduced the LF/HF ratios in both WT ( $2.1 \pm 1.1$ ;  $n = 3$ ) and VACHT KD<sup>HOM</sup> ( $0.9 \pm 0.5$ ;  $n = 3$ ) mice, and these values were not different between genotypes. Taken together, these experiments suggested the possibility that decreased cholinergic tone causes an imbalance of autonomic control of the heart, characterized by altered GPCR activation, with sympathetic tone in VACHT KD<sup>HOM</sup> mice being at a higher level than that in WT mice.

To determine the molecular basis of these changes in GPCR activation, we measured transcript expression levels of muscarinic and adrenergic receptors or associated proteins (such as GPCR kinases [GRKs]). Real-time quantitative PCR analysis of RNA from heart tissue indicated that M<sub>2</sub> muscarinic receptor levels were overexpressed (by 2-fold) in VACHT KD<sup>HOM</sup> hearts (Fig. 6A). In contrast,  $\beta_1$ -adrenergic receptor transcripts were decreased by 41% in VACHT mutant hearts compared to the expression of WT controls (Fig. 6B). This reduction is consistent with attenuated magnitude of ISO-induced increment in  $I_{\text{Ca}}$  in VACHT KD<sup>HOM</sup> cardiomyocytes (Fig. 3B) and the reduced ISO response of VACHT mutants observed *ex vivo* (Fig. 5B). Interestingly, pharmacological restoration of ACh with pyridostigmine treatment for 2 weeks reversed the overexpression of M<sub>2</sub> receptor message in VACHT KD<sup>HOM</sup> hearts, but it did not reverse the decrease in the levels of  $\beta_1$ -adrenergic receptor message. Finally, we examined if we could detect transcripts for muscarinic receptors in isolated adult ventricular cardiomyocytes. We found an increase in M<sub>2</sub> muscarinic receptors in cardiomyocytes similar to what we found in the whole heart, but we also found that M<sub>1</sub> and M<sub>3</sub> transcripts, which have been shown to have a role in inotropic responses (25, 45, 49), were also overexpressed in VACHT KD<sup>HOM</sup> mice (Fig. 6C).

To further confirm if reduced ACh release could alter GPCR message levels, we measured M<sub>2</sub> and  $\beta_1$  receptor messages in recently developed VACHT KO mice (VACHT<sup>del/del</sup> [9]). Homozygous VACHT KO mice are unable to release acetylcholine in response to depolarization and died shortly after birth due to respiratory failure (9). We examined hearts from embryos (day 18.5) of VACHT<sup>del/del</sup> mice and found that they recapitulate the molecular changes in GPCRs levels found in adult VACHT KD<sup>HOM</sup> mice, i.e., mRNA levels of M<sub>2</sub> muscarinic receptors were significantly increased, while the mRNA

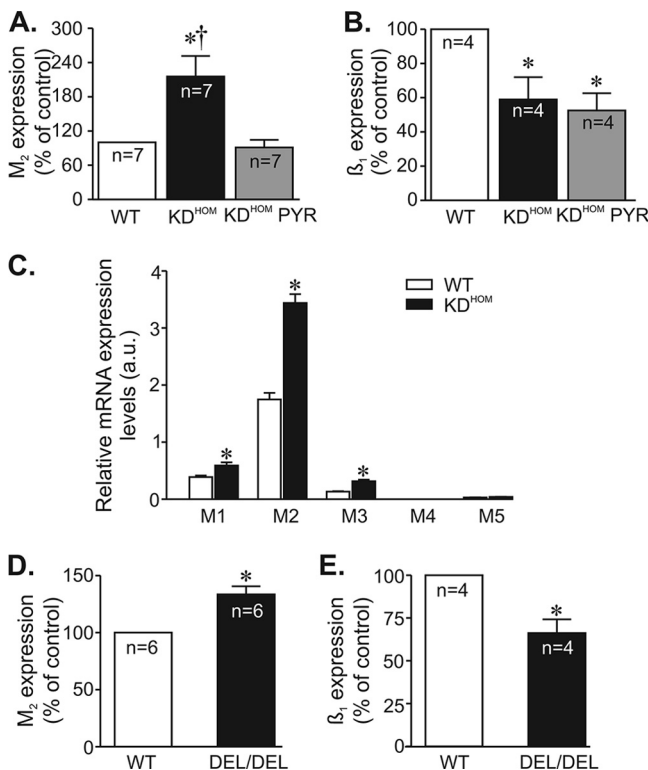


FIG. 6. Effect of VACHT deficiency on M<sub>2</sub> muscarinic and β<sub>1</sub>-adrenergic receptor message levels. M<sub>2</sub> muscarinic and β<sub>1</sub>-adrenergic receptor message levels were determined by qPCR. n, number of heart samples. (A) M<sub>2</sub> mRNA levels were significantly increased in VACHT KD<sup>HOM</sup> hearts. (B) Significant reduction in β<sub>1</sub>-adrenergic receptor mRNA levels was observed in VACHT KD<sup>HOM</sup> hearts. Pyridostigmine treatment prevented the increase in M<sub>2</sub> mRNA levels without affecting β<sub>1</sub>-adrenergic receptor mRNA expression levels in VACHT KD<sup>HOM</sup> hearts. (C) Determination of M<sub>1</sub> to M<sub>5</sub> mRNA expression levels by real-time quantitative PCR in ventricular cardiomyocytes from WT and VACHT KD<sup>HOM</sup> mice. Significant levels of M<sub>1</sub> to M<sub>3</sub> transcripts were detected in cardiomyocytes from WT mice. M<sub>1</sub>, M<sub>2</sub>, and M<sub>3</sub> muscarinic receptor transcript levels were upregulated in VACHT KD<sup>HOM</sup> cardiomyocytes. The bar graph represents data from at least 6 independent experiments. \*, P < 0.05. (D and E) Increased M<sub>2</sub> and reduced β<sub>1</sub>-adrenergic receptor transcript messages are observed in hearts of VACHT knockout mice. \*, P value of <0.05 in comparison with the WT; †, P value of <0.05 in comparison with KD<sup>HOM</sup> mice treated with PYR. n, number of heart samples analyzed.

levels of β<sub>1</sub>-adrenergic receptors were decreased in VACHT<sup>del/del</sup> mice compared to the WT (Fig. 6D and E). Thus, in two distinct strains of mutant mice with altered expression of VACHT, we detected similar gene expression patterns of GPCRs. Alterations in GRK expression levels have the potential to affect GPCR-stimulated biological responses, and GRKs have been shown to be altered in heart failure (40). Therefore, we measured GRK message levels in hearts of VACHT KD<sup>HOM</sup> mice, with particular attention to GRKs that have been previously shown to phosphorylate β-adrenergic or M<sub>2</sub> receptors and participate in receptor desensitization. The message of GRK2, the most-expressed GRK in cardiac tissue, was increased in VACHT KD<sup>HOM</sup> hearts compared to WT controls (by 84%). We also observed a significant increase in GRK5 message levels (by 44%), whereas GRK3 levels were not altered in VACHT KD<sup>HOM</sup> hearts. Moreover, GRK6 expression levels in VACHT

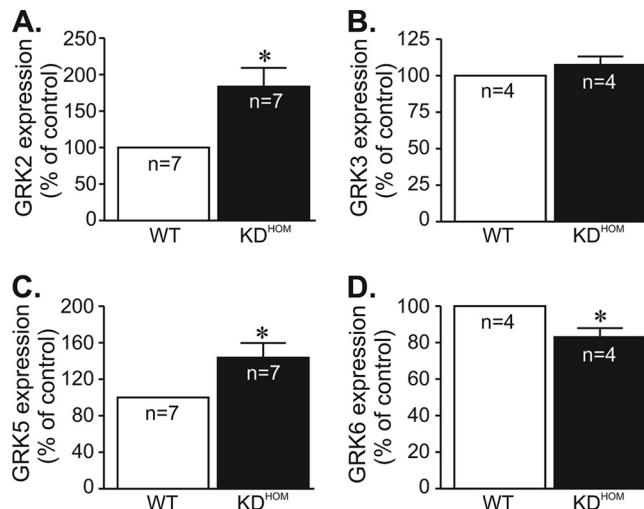


FIG. 7. GRK message expression levels are altered in VACHT mutant hearts. Determination of GRK2 (A), GRK3 (B), GRK5 (C), and GRK6 (D) mRNA expression by real-time quantitative PCR. n, number of hearts analyzed. \*, P < 0.05.

KD<sup>HOM</sup> hearts were reduced by 17% compared to those in WT hearts. Figure 7 summarizes these data. Hence, the alteration in receptor responses may reflect a combination of receptor and GRK changes in hearts of VACHT mutants.

DISCUSSION

In this work, we present evidence that chronic disturbance in cholinergic tone in mutant mice causes changes in cardiac gene expression associated with a molecular remodeling with altered intracellular calcium handling and decreased ventricular function. The dysautonomy due to decreased VACHT expression causes pronounced alterations in autonomic receptor function, with attenuated β<sub>1</sub>-receptor responses, whereas M<sub>2</sub> responses seem exacerbated. Moreover, the cardiac phenotype of VACHT KD<sup>HOM</sup> mice could be reversed by treatment with a cholinesterase inhibitor, pyridostigmine. These data suggest that cholinergic transmission might have unanticipated roles in maintaining ventricular cardiac contractility and that decreased cholinergic tone may contribute to cardiac dysfunction.

Clinical studies have shown that withdrawal of parasympathetic tone precedes sympathetic activation during the development of heart failure (1). For humans, spectral analysis suggests that aging, one of the major risk factors for heart failure, decreases parasympathetic drive (11). Animal studies further corroborated these data by showing autonomic imbalance in the early stage of experimental heart failure in dogs (22). Thus, dysautonomy plays important roles in pathological changes in the heart (37). However, given that genetic interference in the presynaptic cholinergic system is usually fatal, it has been difficult to chronically disturb the cholinergic autonomic nervous system to understand if acetylcholine plays any unanticipated roles in cardiac contractility.

VACHT presence in synaptic vesicles is fundamental for evoked release of ACh, as VACHT KO mice cannot release this neurotransmitter (9), and the VACHT KD<sup>HOM</sup> mice,

which present reduced VAcHT expression, show reduced ACh packing in synaptic vesicles (41). It is likely that both the sympathetic and parasympathetic nervous systems are affected in VAcHT KD<sup>HOM</sup> mice, since both depend on preganglionic cholinergic neurotransmission, albeit the parasympathetic nervous system should be hit twice due to its postganglionic cholinergic phenotype. We favor the possibility that dysautonomy caused by decreased cholinergic tone results in imbalance of autonomic control of the heart in mutant mice, based on the following evidence. First, it is known that at room temperature (25°C), the sympathetic drive predominates in mice and keeps their heart rate high (18). We found that heart rates were identical in the two genotypes despite a substantial decrease in  $\beta_1$ -receptor expression and function in VAcHT KD<sup>HOM</sup> mice, suggesting that *in vivo*, the sympathetic nervous system needed to be overactivated in VAcHT KD<sup>HOM</sup> mice in order to maintain the basal HR at levels that were similar to those of the WT. Second, the changes in  $\beta_1$ -receptor expression and GRKs observed for VAcHT KD<sup>HOM</sup> mice are similar to those seen in models of adrenergic overactivation (19, 39). Third, the effect of sympathetic blockade on changes in HR responses were significantly enhanced in VAcHT KD<sup>HOM</sup> mice, suggesting an important sympathetic component to maintenance of normal values of heart rate in the mutant mice. It is therefore conceivable that dysautonomy caused by reduced cholinergic function in VAcHT mutants favors an increased sympathetic tone in these mice. The HR variability analysis conducted here supports this conclusion.

An intriguing observation is the reduced heart rate found in Langerdorff preparation-perfused hearts of mutant mice. This finding agrees with the results of autonomic blockage *in vivo* showing a reduced intrinsic heart rate in VAcHT KD<sup>HOM</sup> mice. It is likely that these results reflect reduced sinoatrial node action potential firing in mutant mice. Future studies will be needed to determine the ionic and molecular bases of these changes.

Our findings contrast in part with the results obtained with another model of cholinergic dysfunction, the M<sub>2</sub>-AChR knockout mice (26). In spite of the similar *in vivo* HRs of the VAcHT KD<sup>HOM</sup> and M<sub>2</sub>-AChR knockout mice compared to their respective controls, these two mouse strains presented distinct degrees of cardiac dysfunction and remodeling. Since most of the major cardiac changes observed in VAcHT KD<sup>HOM</sup> mice can be attributed to the reduced cholinergic tone, it seems reasonable to have expected that the same array of changes would be observed in the M<sub>2</sub>-AChR knockout mice. One potential explanation for these phenotypic distinctions is the degree of activation of  $\beta$ -adrenergic and muscarinic signaling. Whereas  $\beta$ -adrenergic responses were significantly altered in VAcHT mutants, this signaling pathway was preserved in M<sub>2</sub>-AChR knockout mice (26). Moreover, VAcHT mice presented exacerbated M<sub>2</sub> responses, in contrast to M<sub>2</sub>-AChR knockout mice, in which M<sub>2</sub> responses were absent (26). There is another consideration: the existence of other types of muscarinic receptors in the heart, albeit with lower levels of expression, has been reported (44, 49). Indeed, we could also detect M<sub>1</sub> and M<sub>3</sub> muscarinic receptor messages in ventricular cardiomyocytes, and their expression was elevated in VAcHT KD<sup>HOM</sup> mice. It is surprising that M<sub>2</sub>, M<sub>1</sub>, and M<sub>3</sub> receptors are all upregulated in ventricular myocytes from VAcHT mu-

tants, even though parasympathetic fibers are not abundant in ventricles of rodents (30). Therefore, ACh may control ventricular cell function by mechanisms that are not characterized yet, and disturbance of VAcHT expression can interfere with ventricular function. In fact, the possibility that cardiomyocytes express presynaptic cholinergic proteins has been raised recently (23).

It is well established that acetylcholine controls atrial function, with predominant roles in maintaining heart rate and action potential conduction. Unexpectedly, we found that altered cholinergic tone also provokes profound effects on ventricular cardiomyocytes. The array of cellular changes included Ca<sup>2+</sup> signaling dysfunction and altered GPCR function. Interestingly, these changes occurred without altering I<sub>Ca</sub> density or action potential properties. Overall, the cardiac remodeling observed for VAcHT mutant mice resembles in many aspects the remodeling process observed for animal models of heart failure with sympathetic overdrive (7, 19, 39). Therefore, we suggest that the autonomic imbalance in the sympathetic direction in VAcHT mutants, with decreased parasympathetic activity, can largely explain the development of ventricular dysfunction in these mice.

It is not clear at the moment if the overexpression of M<sub>2</sub> muscarinic receptors contributes to the VAcHT cardiac phenotype. We found that hearts from VAcHT mutants were more sensitive to the bradycardic effects of ACh, suggesting the presence of increased functional M<sub>2</sub> receptors in these hearts. It is well known that M<sub>2</sub> receptors couple to the Gi/0 family of G proteins (27) to inhibit adenylyl cyclase; therefore, it is likely that M<sub>2</sub> overexpression may also contribute to the impaired  $\beta_1$  response in VAcHT mutant hearts. Consistent with this notion, improvement in ventricular function following pyridostigmine treatment of VAcHT mice occurred in spite of reduced  $\beta_1$ -receptor mRNA levels. It remains to be determined if attenuation of  $\beta_1$ -adrenergic receptor mRNA in this model is a late event that may require more-prolonged pyridostigmine treatment. Levels of GRK2 are elevated in different models of heart failure characterized by enhanced chronic neurohumoral stimulation, in which they contribute to  $\beta_1$ -adrenergic receptor attenuation (39). Consistent with this notion, we found increased GRK2 levels in the VAcHT mutant model of cholinergic deficiency. Our results also demonstrated an upregulation of GRK5 in VAcHT mutant hearts. Recently, Martini and collaborators (31) have characterized a new role for GRK5 as a nuclear histone deacetylase (HDAC) kinase with a key role in maladaptive cardiac hypertrophy. In this context, nuclear accumulation of GRK5 correlates with enhanced ventricular expression of the hypertrophy-associated fetal gene program (31). It is interesting that 3-month-old VAcHT KD<sup>HOM</sup> mice had no sign of cardiac hypertrophy, although they showed increased levels of ANF and  $\beta$ -MHC transcripts. However, it is important to mention that ventricular expression of these markers is not always associated with cardiac hypertrophy (38, 48). In contrast, 6-month-old mice presented concentric hypertrophy, suggesting that cardiac dysfunction is progressive in VAcHT mutant hearts as a result of chronic depressed cholinergic drive with age. It remains to be determined whether aged VAcHT KD<sup>HOM</sup> mice will present further features of heart failure. Another critical aspect of cardiac dysfunction in heart failure is ventricular dyssynchrony.

In fact, ventricular dyssynchrony has been shown to have deleterious effects on cardiac function resulting in contractile inefficiency and increased mortality (46). It remains to be determined whether VACHT KD<sup>DOM</sup> mice present ventricular dyssynchrony.

Taken together, our experiments indicate that dysautonomy causes profound changes in gene expression, suggesting that the balanced long-term responses of GPCRs are fundamental to maintain cardiac gene expression to maintain normal heart function. Our data also add to recent evidence suggesting that therapies aimed at enhancing parasympathetic activation may have positive effects on patients with heart failure (16, 43, 47).

#### ACKNOWLEDGMENTS

We thank Sanda Raulic and Jue Fan for mouse husbandry and genotyping at the University of Western Ontario, Richard Premont and Raul Gainetdinov (Duke University Medical Center) for advice on GRK PCR, and Brian Collier (McGill University) and R. Jane Rylett (University of Western Ontario) for comments on earlier versions of the manuscript.

This work was supported by the Heart and Stroke Foundation of Ontario (grant NA 6656 to R.G., S.G., V.F.P., and M.A.M.P.), CIHR (grants MOP-82756 to R.G. and MOP-89919 to V.F.P. and M.A.M.P.), NIH-Fogarty grant R21 TW007800-02 (to M.A.M.P., V.F.P., and M.G.C.), PRONEX-FAPEMIG (to M.A.M.P., V.F.P., and S.G.), CNPq (to S.G., J.S.C., V.F.P., and M.A.M.P.), FAPEMIG, and Instituto do Milenio Toxins/MCT (to M.V.G., M.A.M.P., V.F.P., A.P.A., and S.G.). R.P. and C.A.S.M. received postdoctoral fellowships from the Department of Foreign Affairs and International Trade (Canada). R.G. is supported by a New Investigator Award from the Heart and Stroke Foundation of Canada.

#### REFERENCES

- Amorim, D. S., H. J. Dargie, K. Heer, M. Brown, D. Jenner, E. G. Olsen, P. Richardson, and J. F. Goodwin. 1981. Is there autonomic impairment in congestive (dilated) cardiomyopathy? *Lancet* **i**:525–527.
- Bartholomeu, J. B., A. S. Vanzelli, N. P. Rolim, J. C. Ferreira, L. R. Bechara, L. Y. Tanaka, K. T. Rosa, M. M. Alves, A. Medeiros, K. C. Mattos, M. A. Coelho, M. C. Irigoyen, E. M. Krieger, J. E. Krieger, C. E. Negrao, P. R. Ramires, S. Guatimosim, and P. C. Brum. 2008. Intracellular mechanisms of specific beta-adrenoceptor antagonists involved in improved cardiac function and survival in a genetic model of heart failure. *J. Mol. Cell. Cardiol.* **45**:240–249.
- Bers, D. M. 2006. Altered cardiac myocyte Ca regulation in heart failure. *Physiology (Bethesda)* **21**:380–387.
- Bers, D. M. 2002. Cardiac excitation-contraction coupling. *Nature* **415**:198–205.
- Brandon, E. P., W. Lin, K. A. D'Amour, D. P. Pizzo, B. Dominguez, Y. Sugiura, S. Thode, C. P. Ko, L. J. Thal, F. H. Gage, and K. F. Lee. 2003. Aberrant patterning of neuromuscular synapses in choline acetyltransferase-deficient mice. *J. Neurosci.* **23**:539–549.
- Castro, C. H., R. A. Santos, A. J. Ferreira, M. Bader, N. Alenina, and A. P. Almeida. 2005. Evidence for a functional interaction of the angiotensin-(1-7) receptor Mas with AT1 and AT2 receptors in the mouse heart. *Hypertension* **46**:937–942.
- Chakir, K., S. K. Daya, T. Aiba, R. S. Tunin, V. L. Dimaano, T. P. Abraham, K. M. Jaques-Robinson, E. W. Lai, K. Pacak, W. Z. Zhu, R. P. Xiao, G. F. Tomaselli, and D. A. Kass. 2009. Mechanisms of enhanced beta-adrenergic reserve for cardiac resynchronization therapy. *Circulation* **119**:1231–1240.
- Cruz, J. S., and H. Matsuda. 1994. Depressive effects of arenobufagin on the delayed rectifier K<sup>+</sup> current of guinea-pig cardiac myocytes. *Eur. J. Pharmacol.* **266**:317–325.
- de Castro, B. M., X. De Jaeger, C. Martins-Silva, R. D. Lima, E. Amaral, C. Menezes, P. Lima, C. M. Neves, R. G. Pires, T. W. Gould, I. Welch, C. Kushmerick, C. Guatimosim, I. Izquierdo, M. Cammarota, R. J. Rylett, M. V. Gomez, M. G. Caron, R. W. Oppenheim, M. A. Prado, and V. F. Prado. 2009. The vesicular acetylcholine transporter is required for neuromuscular development and function. *Mol. Cell Biol.* **29**:5238–5250.
- de Castro, B. M., G. S. Pereira, V. Magalhaes, J. I. Rossato, X. De Jaeger, C. Martins-Silva, B. Leles, P. Lima, M. V. Gomez, R. R. Gainetdinov, M. G. Caron, I. Izquierdo, M. Cammarota, V. F. Prado, and M. A. Prado. 2009. Reduced expression of the vesicular acetylcholine transporter causes learning deficits in mice. *Genes Brain Behav.* **8**:23–35.
- De Meersman, R. E., and P. K. Stein. 2007. Vagal modulation and aging. *Biol. Psychol.* **74**:165–173.
- Dhein, S., C. J. van Koppen, and O. E. Brodde. 2001. Muscarinic receptors in the mammalian heart. *Pharmacol. Res.* **44**:161–182.
- Duprez, D. A. 2008. Cardiac autonomic imbalance in pre-hypertension and in a family history of hypertension. *J. Am. Coll. Cardiol.* **51**:1902–1903.
- Ferreira, A. J., T. L. Oliveira, M. C. Castro, A. P. Almeida, C. H. Castro, M. V. Caliari, E. Gava, G. T. Kitten, and R. A. Santos. 2007. Isoproterenol-induced impairment of heart function and remodeling are attenuated by the nonpeptide angiotensin-(1-7) analogue AVE 0991. *Life Sci.* **81**:916–923.
- Floras, J. S. 1993. Clinical aspects of sympathetic activation and parasympathetic withdrawal in heart failure. *J. Am. Coll. Cardiol.* **22**:72A–84A.
- Freeling, J., K. Wattier, C. LaCroix, and Y. F. Li. 2008. Neostigmine and pilocarpine attenuated tumour necrosis factor alpha expression and cardiac hypertrophy in the heart with pressure overload. *Exp. Physiol.* **93**:75–82.
- Funakoshi, H., T. Kubota, N. Kawamura, Y. Machida, A. M. Feldman, H. Tsutsui, H. Shimokawa, and A. Takeshita. 2002. Disruption of inducible nitric oxide synthase improves beta-adrenergic inotropic responsiveness but not the survival of mice with cytokine-induced cardiomyopathy. *Circ. Res.* **90**:959–965.
- Gehrmann, J., P. E. Hammer, C. T. Maguire, H. Wakimoto, J. K. Triedman, and C. I. Berul. 2000. Phenotypic screening for heart rate variability in the mouse. *Am. J. Physiol. Heart Circ. Physiol.* **279**:H733–H740.
- Grassi, G., G. Seravalle, F. Quarti-Trevano, and R. Dell'oro. 2009. Sympathetic activation in congestive heart failure: evidence, consequences and therapeutic implications. *Curr. Vasc. Pharmacol.* **7**:137–145.
- Gros, R., X. You, L. L. Baggio, M. G. Kabir, A. M. Sadi, I. N. Mungrue, T. G. Parker, Q. Huang, D. J. Drucker, and M. Husain. 2003. Cardiac function in mice lacking the glucagon-like peptide-1 receptor. *Endocrinology* **144**:2242–2252.
- Guatimosim, S., E. A. Sobie, C. J. dos Santos, L. A. Martin, and W. J. Lederer. 2001. Molecular identification of a TTX-sensitive Ca(2+) current. *Am. J. Physiol. Cell Physiol.* **280**:C1327–C1339.
- Ishise, H., H. Asanoi, S. Ishizaka, S. Joho, T. Kameyama, K. Umeno, and H. Inoue. 1998. Time course of sympathovagal imbalance and left ventricular dysfunction in conscious dogs with heart failure. *J. Appl. Physiol.* **84**:1234–1241.
- Kakinuma, Y., T. Akiyama, and T. Sato. 2009. Cholinoceptive and cholinergic properties of cardiomyocytes involving an amplification mechanism for vagal efferent effects in sparsely innervated ventricular myocardium. *FEBS J.* **276**:5111–5125.
- Kent, K. M., S. E. Epstein, T. Cooper, and D. M. Jacobowitz. 1974. Cholinergic innervation of the canine and human ventricular conducting system. Anatomic and electrophysiologic correlations. *Circulation* **50**:948–955.
- Korth, M., V. K. Sharma, and S. S. Sheu. 1988. Stimulation of muscarinic receptors raises free intracellular Ca<sup>2+</sup> concentration in rat ventricular myocytes. *Circ. Res.* **62**:1080–1087.
- LaCroix, C., J. Freeling, A. Giles, J. Wess, and Y. F. Li. 2008. Deficiency of M2 muscarinic acetylcholine receptors increases susceptibility of ventricular function to chronic adrenergic stress. *Am. J. Physiol. Heart Circ. Physiol.* **294**:H810–H820.
- Lanzafame, A. A., A. Christopoulos, and F. Mitchelson. 2003. Cellular signaling mechanisms for muscarinic acetylcholine receptors. *Receptors Channels* **9**:241–260.
- Li, M., C. Zheng, T. Sato, T. Kawada, M. Sugimachi, and K. Sunagawa. 2004. Vagal nerve stimulation markedly improves long-term survival after chronic heart failure in rats. *Circulation* **109**:120–124.
- Lloyd-Mostyn, R. H., and P. J. Watkins. 1975. Defective innervation of heart in diabetic autonomic neuropathy. *Br. Med. J.* **3**:15–17.
- Mabe, A. M., J. L. Hoard, M. M. Duffour, and D. B. Hoover. 2006. Localization of cholinergic innervation and neurturin receptors in adult mouse heart and expression of the neurturin gene. *Cell Tissue Res.* **326**:57–67.
- Martini, J. S., P. Raake, L. E. Vinge, B. DeGeorge, Jr., J. K. Chuprun, D. M. Harris, E. Gao, A. D. Eckhart, J. A. Pitcher, and W. J. Koch. 2008. Uncovering G protein-coupled receptor kinase-5 as a histone deacetylase kinase in the nucleus of cardiomyocytes. *Proc. Natl. Acad. Sci. U. S. A.* **105**:12457–12462.
- Misgeld, T., R. W. Burgess, R. M. Lewis, J. M. Cunningham, J. W. Lichtman, and J. R. Sanes. 2002. Roles of neurotransmitter in synapse formation: development of neuromuscular junctions lacking choline acetyltransferase. *Neuron* **36**:635–648.
- Mungrue, I. N., R. Gros, X. You, A. Pirani, A. Azad, T. Csont, R. Schulz, J. Butany, D. J. Stewart, and M. Husain. 2002. Cardiomyocyte overexpression of iNOS in mice results in peroxynitrite generation, heart block, and sudden death. *J. Clin. Invest.* **109**:735–743.
- Nagata, K., C. Ye, M. Jain, D. S. Milstone, R. Liao, and R. M. Mortensen. 2000. Galpha(12) but not Galpha(13) is required for muscarinic inhibition of contractility and calcium currents in adult cardiomyocytes. *Circ. Res.* **87**:903–909.
- Okoshi, K., M. Nakayama, X. Yan, M. P. Okoshi, A. J. Schuldt, M. A. Marchionni, and B. H. Lorell. 2004. Neuregulins regulate cardiac parasympathetic activity: muscarinic modulation of beta-adrenergic activity in myocytes from mice with neuregulin-1 gene deletion. *Circulation* **110**:713–717.
- Oliveira, F. A., S. Guatimosim, C. H. Castro, D. T. Galan, S. Lauton-Santos,

- A. M. Ribeiro, A. P. Almeida, and J. S. Cruz. 2007. Abolition of reperfusion-induced arrhythmias in hearts from thiamine-deficient rats. *Am. J. Physiol. Heart Circ. Physiol.* **293**:H394–H401.
37. Olshansky, B., H. N. Sabbah, P. J. Hauptman, and W. S. Colucci. 2008. Parasympathetic nervous system and heart failure: pathophysiology and potential implications for therapy. *Circulation* **118**:863–871.
  38. Pandya, K., H. S. Kim, and O. Smithies. 2006. Fibrosis, not cell size, delineates beta-myosin heavy chain reexpression during cardiac hypertrophy and normal aging in vivo. *Proc. Natl. Acad. Sci. U. S. A.* **103**:16864–16869.
  39. Penela, P., C. Murga, C. Ribas, A. S. Tutor, S. Peregrin, and F. Mayor, Jr. 2006. Mechanisms of regulation of G protein-coupled receptor kinases (GRKs) and cardiovascular disease. *Cardiovasc. Res.* **69**:46–56.
  40. Petrofski, J. A., and W. J. Koch. 2003. The beta-adrenergic receptor kinase in heart failure. *J. Mol. Cell. Cardiol.* **35**:1167–1174.
  41. Prado, V. F., C. Martins-Silva, B. M. de Castro, R. F. Lima, D. M. Barros, E. Amaral, A. J. Ramsey, T. D. Sotnikova, M. R. Ramirez, H. G. Kim, J. I. Rossato, J. Koenen, H. Quan, V. R. Cota, M. F. Moraes, M. V. Gomez, C. Guatimosim, W. C. Wetsel, C. Kushmerick, G. S. Pereira, R. R. Gainetdinov, I. Izquierdo, M. G. Caron, and M. A. Prado. 2006. Mice deficient for the vesicular acetylcholine transporter are myasthenic and have deficits in object and social recognition. *Neuron* **51**:601–612.
  42. Rota, M., T. Hosoda, A. De Angelis, M. L. Arcarese, G. Esposito, R. Rizzi, J. Tillmanns, D. Tugal, E. Musso, O. Rimoldi, C. Bearzi, K. Urbanek, P. Anversa, A. Leri, and J. Kajstura. 2007. The young mouse heart is composed of myocytes heterogeneous in age and function. *Circ. Res.* **101**:387–399.
  43. Serra, S. M., R. V. Costa, R. R. Teixeira De Castro, S. S. Xavier, and A. C. Nobrega. 2009. Cholinergic stimulation improves autonomic and hemodynamic profile during dynamic exercise in patients with heart failure. *J. Card. Fail.* **15**:124–129.
  44. Sharma, V. K., H. M. Colecraft, L. E. Rubin, and S. S. Sheu. 1997. Does mammalian heart contain only the M2 muscarinic receptor subtype? *Life Sci.* **60**:1023–1029.
  45. Sharma, V. K., H. M. Colecraft, D. X. Wang, A. I. Levey, E. V. Grigorenko, H. H. Yeh, and S. S. Sheu. 1996. Molecular and functional identification of m1 muscarinic acetylcholine receptors in rat ventricular myocytes. *Circ. Res.* **79**:86–93.
  46. Spragg, D. D., and D. A. Kass. 2006. Pathobiology of left ventricular dyssynchrony and resynchronization. *Prog. Cardiovasc. Dis.* **49**:26–41.
  47. Thayer, J. F., and R. D. Lane. 2007. The role of vagal function in the risk for cardiovascular disease and mortality. *Biol. Psychol.* **74**:224–242.
  48. Vikstrom, K. L., T. Bohlmeier, S. M. Factor, and L. A. Leinwand. 1998. Hypertrophy, pathology, and molecular markers of cardiac pathogenesis. *Circ. Res.* **82**:773–778.
  49. Wang, Z., H. Shi, and H. Wang. 2004. Functional M3 muscarinic acetylcholine receptors in mammalian hearts. *Br. J. Pharmacol.* **142**:395–408.
  50. Wu, J. S., F. H. Lu, Y. C. Yang, T. S. Lin, J. J. Chen, C. H. Wu, Y. H. Huang, and C. J. Chang. 2008. Epidemiological study on the effect of pre-hypertension and family history of hypertension on cardiac autonomic function. *J. Am. Coll. Cardiol.* **51**:1896–1901.
  51. Yang, L. L., R. Gros, M. G. Kabir, A. Sadi, A. I. Gotlieb, M. Husain, and D. J. Stewart. 2004. Conditional cardiac overexpression of endothelin-1 induces inflammation and dilated cardiomyopathy in mice. *Circulation* **109**:255–261.